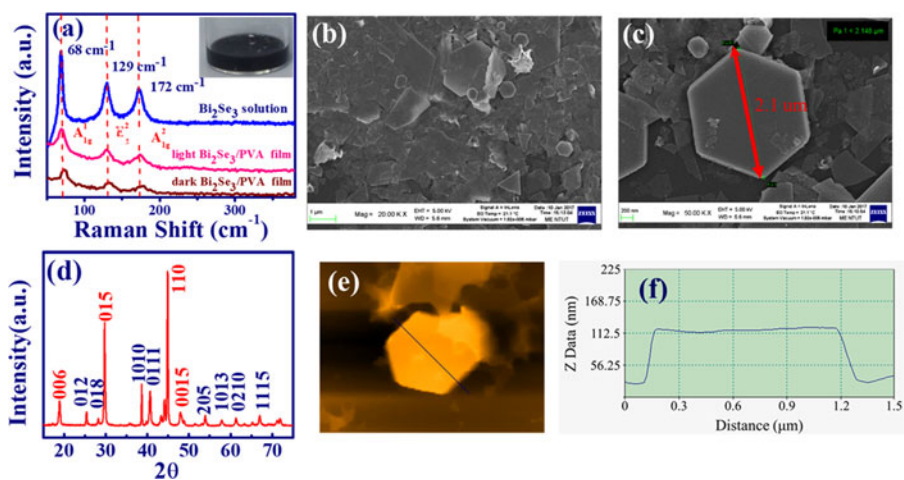


Q-Switched Pulse and Mode-Locked Pulse Generation From a Yb^{3+} -Doped Fiber Laser Based on Bi_2Se_3

Volume 10, Number 3, June 2018

Ja-Hon Lin
Guan-Hao Huang
Chu-Hsiang Ou
Kuan-Chin Che
Wei-Rein Liu
Shwu-Yun Tasy
Yao-Hui Chen



DOI: 10.1109/JPHOT.2018.2823785

1943-0655 © 2018 IEEE

Q-Switched Pulse and Mode-Locked Pulse Generation From a Yb³⁺-Doped Fiber Laser Based on Bi₂Se₃

Ja-Hon Lin ¹, Guan-Hao Huang,¹ Chu-Hsiang Ou,¹
Kuan-Chin Che,¹ Wei-Rein Liu,² Shwu-Yun Tasy,¹ and Yao-Hui Chen¹

¹Department of Electro-Optical Engineering and Institute of Electro-Optical Engineering,
National Taipei University of Technology, Taipei 10608, Taiwan

²National Synchrotron Radiation Research Center, Hsinchu 30076, Taiwan

DOI:10.1109/JPHOT.2018.2823785

1943-0655 © 2018 IEEE. Translations and content mining are permitted for academic research only.

Personal use is also permitted, but republication/redistribution requires IEEE permission.

See http://www.ieee.org/publications_standards/publications/rights/index.html for more information.

Manuscript received February 10, 2018; revised March 28, 2018; accepted March 29, 2018. Date of publication April 6, 2018; date of current version May 3, 2018. This work was supported by the Ministry of Science and Technology Taiwan under Grant MOST 105-2112-M-027-001-MY3. Corresponding author: Ja-Hon Lin (e-mail jhlin@ntut.edu.tw).

Abstract: The Q-switched pulse and mode-locked pulse were investigated in an all-normal dispersion Yb-doped fiber laser (YDFL) based on the topological insulators (TIs) with mixing of polyvinyl alcohol (PVA) to produce Bi₂Se₃/PVA film or deposition on the end facet of fiber to manufacture TI-compatible fiber. Through the dark Bi₂Se₃/PVA films with large nonsaturable loss, the YDFL was operated in the Q-switched state. The repetition rate and the duration of the Q-switched pulses increased and declined, respectively, with the pump power to show 2.2 μ s duration and 137.8 kHz repetition rate at the highest pump power. Moreover, the mode-locked pulses, with a 16 MHz repetition rate and 380 ps pulsewidth, were generated at high pump power by using the light Bi₂Se₃/PVA film. By means of a Bi₂Se₃ compatible fiber, through optical deposition of the Bi₂Se₃ nanoplatelets on the end facet of the fiber, the mode-locked YDFL was generated at low-threshold pump power and revealed more stabilized operation state up to two hours.

Index Terms: Q-switched laser, mode-locked laser, Yb³⁺-doped fiber laser, topological insulators.

1. Introduction

Nowadays, passively mode-locked fiber lasers (PML-FLs) have been extensively investigated and widely used in various fields because of their excellent properties such as robust operation, compact size, and low production cost in comparison to other solid state or gas lasers. In order to achieve stabilized passively mode-locking in fiber lasers, artificial saturable absorbers (SAs) such as the nonlinear polarization rotation [1]–[3], nonlinear loop mirror [4], and nonlinear amplifying loop mirror, etc., have been reported in operation at high pump power. In addition, many devices or nanomaterials, such as semiconductor saturable absorber mirrors (SESAMs) [5], carbon nanotubes [6], graphene [7], [8], graphene oxide [9], [10], etc., have been employed inside the cavity of fiber lasers as the SAs to produce the mode-locked pulses. Although the SESAM has been widely adopted in PML-FLs for the generation of short and robust pulses, the fabrication and packaging technology are complex and expensive, and the operation bandwidth is relatively narrow. In recent years, many studies have focused on the investigation and production of various nanomaterial-based SAs, because

of their superior optical properties, including ultrafast recovery time, controllable modulation depth, and easy fabrication, which function as ultrafast optical switching for short pulse generation in PML-FLs. In particular, graphene and graphene oxide, two types of Dirac nanomaterial, have been demonstrated as superior SAs for mode-locked lasers, but they possess low modulation depth [11], [12].

Recently, topological insulators (TIs), another type of Dirac nanoscale material, have attracted considerable attention in condensed matter physics, and revealed a characteristic with a robust metallic surface state and a narrow band-gap bulk state [13]–[16]. Besides, they are also promising devices for the generation of ultrashort pulses in near- to mid-IR fiber lasers due to their excellent wideband saturable absorption property. Different kinds of SAs, such as the Bi_2Se_3 , Bi_2Te_3 and Sb_2Te_3 nano-plates (NPs) or nanosheets, have been produced via the solvothermal method or liquid phase exfoliation method [17]–[20]. Among all the TIs, the Bi_2Se_3 has been noted because of its greater band gap of ~ 0.3 eV and can be considered as a promising optical material for room-temperature applications. In a previous report, Bi_2Se_3 /PVA films, prepared by mixing Bi_2Se_3 NPs or nanosheets with Polyvinyl alcohol (PVA), were sandwiched between two fiber connectors inside the laser cavity to generate mode-locked pulse [21]–[24] or Q-switched pulse in Er-doped fiber lasers (EDFLs) [25]–[27].

In contrast to the EDFLs, the pulse dynamics of the ytterbium-doped fiber lasers (YDFLs) by using the Bi_2Se_3 as a SA are rare reported. Luo *et al.* demonstrated the passive Q-switching from a YDFL with a linear cavity configuration through the TI compatible fiber, which was manufactured by the optical deposition of few-layer Bi_2Se_3 on the end facet of fiber [28]. In addition, the Bi_2Se_3 film, fabricated by using the filter paper transfer method, was also adopted to generate the ML pulse in YDFL [29]. Nevertheless, it is seldom to discuss the generated mechanism of Q-switched pulse or mode-locked pulse that is related to the non-saturable loss of SA. In this report, we produced the Bi_2Se_3 /PVA films with high and low transmittance by drying the mixed solution comprising Bi_2Se_3 NPs and PVA powders at the different locations of the standard cell. After insertion of the dark or light Bi_2Se_3 /PVA films inside the laser cavity, the Q-switched pulse or passively mode-locked pulse can be generated, respectively. In addition, the TI compatible fiber has also been used in PML-YDFLs with more stabilized operation performance.

2. Preparation of Bi_2Se_3 Nano-Platelets and Experimental Setup

In this work, the Bi_2Se_3 NPs were synthesized via the polyol method [25]. First, 0.6 g $\text{Bi}(\text{NO}_3)_3 \cdot 5\text{H}_2\text{O}$, 0.3 g sodium selenite, 1.32 g polyvinyl pyrrolidone, and 60 mL ethylene glycol (EG) were mixed in a 250.0 mL two-neck flask that was placed on a heating mantle and connected with a reflux condenser. The temperature of the solution was increased to 190 °C under constant stirring by a Teflon-coated magnetic stirring bar. In order to produce regular Bi_2Se_3 NPs, the chemical reactions were continuous within 6 hours. The cooled and reacted products were dissolved into the isopropyl alcohol (IPA) and then ultrasonically agitated for 10 minutes. Then, the reacted solution was poured into 10 mL tubes and centrifuged for 10 minutes at 6,000 rpm to separate the different sizes of NPs and remove residual EG. The process of washing and centrifugation was repeated several times to remove the large size NPs. Finally, we dried the reacted products inside the culture dish for 6 hours to generate NPs. In order to manufacture the Bi_2Se_3 /PVA film, the NPs were added into 10 ml DI water and ultrasonically agitated for 4.5 hours. Then, we uniformly mixed PVA powders into the Bi_2Se_3 solution and stirred with a Teflon-coated magnetic stirring bar at a temperature of 90 °C in a vessel for 4 hours.

Fig. 1(a) shows the room temperature Raman spectrum of the Bi_2Se_3 dispersed solution (blue line), by dissolving Bi_2Se_3 NPs in the DI water (the picture shown in the inset of Fig. 1(a)), as well as light (pink line) and dark (brown line) Bi_2Se_3 /PVA films using a 532 nm CW laser as excitation. Three typical Raman peaks of Bi_2Se_3 NPs located at ~ 68 cm^{-1} , ~ 129 cm^{-1} , 172 cm^{-1} , respectively, correspond to the out-plane vibrational mode A_{1g}^1 , in-plane vibrational mode E_g^2 , and the out-plane vibrational mode A_{1g}^2 of Se-Bi-Se-Bi-Se lattice vibration. Owing to the light scattering, the signal

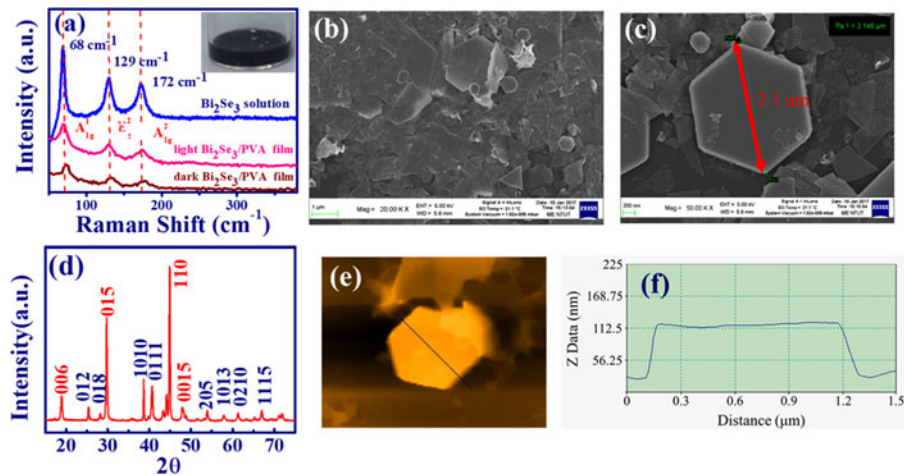


Fig. 1. (a) Raman spectrum of Bi_2Se_3 dispersed solution (blue line), as well as light (pink line) and dark (brown line) $\text{Bi}_2\text{Se}_3/\text{PVA}$ films (brown). (Inset: photograph of Bi_2Se_3 solution by dissolving NPs in DI water.) (b) The enlarged 20 K SEM, and (c) the enlarged 50 K SEM of TI: Bi_2Se_3 NPs. (d) XRD patterns of Bi_2Se_3 powder. (e) The AFM image and (f) the thickness of single TI: Bi_2Se_3 NP.

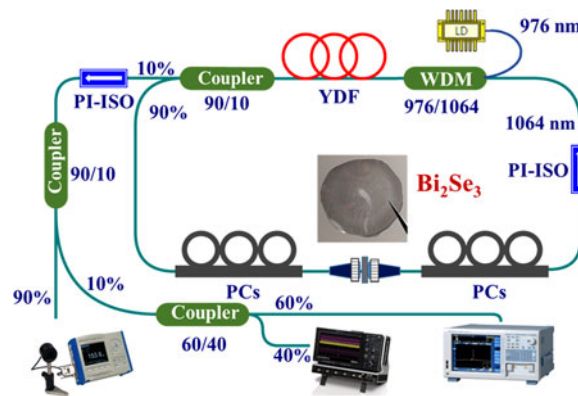


Fig. 2. The schematic diagram of the all normal-dispersion PML-YDFL by using TI-SA with ring cavity configuration.

from the rough surface of the bright and dark films are smaller than the NPs in dispersed solution. The enlarged 20 K SEM image of the Bi_2Se_3 NPs in Fig. 1(b) indicates that the nano-material has a quasi-two-dimensional structure with regular hexagonal shape. The enlarged 50 K SEM image in Fig. 1(c) shows that the planar dimensional Bi_2Se_3 NPs possess hexagonal morphologies of around $2.1 \mu\text{m}$. Fig. 1(d) shows the XRD pattern of the Bi_2Se_3 NPs collected by using MYTHEN 24 K detector at TPS 09A (Taiwan Photon Source), in which the diffraction peaks from each sample can be well indexed to exhibit a rhombohedral structure with no detectable impurities of other phases in comparison with the JCPDS data card No. 33-0214. The AFM image and the corresponding thickness of Bi_2Se_3 NPs measured by a commercial closed-loop-scanner scanning probe microscopy (Innova, Veeco) at NSRRC are shown in the Fig. 1(e) and (f).

The schematic diagram of the ring cavity configuration YDFL is shown in Fig. 2. A pigtail laser diode (LD) with emission wavelength of around 976 nm was used as a pump source that was coupled inside the laser cavity through a wavelength division multiplexer (WDM). The laser cavity comprised of a 140 cm long Yb-doped fiber (YDF, with absorption around 280 dB/m at 920 nm) as a gain fiber, a 90/10 output coupler, two polarization controllers (PCs) for adjusting the polarization

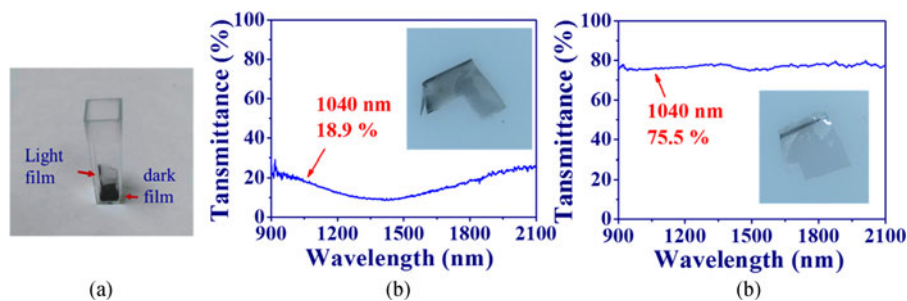


Fig. 3. (a) Picture of $\text{Bi}_2\text{Se}_3/\text{PVA}$ film dried onto the standard cell. The transmission spectrum for the (b) dark and (c) light $\text{Bi}_2\text{Se}_3/\text{PVA}$ film. Insets of figures (b) and (c) show photographs of these two films.

inside the laser cavity, and a polarization independent isolator (PI-ISO) to ensure uni-directional propagation inside the laser cavity. In order to generate the Q-switched pulses and mode-locked pulses inside the laser cavity, a small piece of $\text{Bi}_2\text{Se}_3/\text{PVA}$ film was sandwiched between two end facets of the fibers. The laser beam inside cavity was divided by the 90/10 coupler, in which 90% of the output light was measured by a power meter to monitor the output power or the autocorrelator to obtain the pulsewidth. The residual power (10% from 90/10 coupler) was divided by the other 60/40 coupler and then measured by an optical spectrum analyzer (OSA, AQ 6370, Yokogawa Inc.) or detected by a high speed detector (ET-3010, EOT Inc.), and then displayed on the oscilloscope (WaveRunner 620 Zi, LeCroy Inc.) to monitor the pulse dynamics of YDFL.

3. Results and Discussion

3.1 Short Pulse Generation by $\text{Bi}_2\text{Se}_3/\text{PVA}$ Films

In order to produce the $\text{Bi}_2\text{Se}_3/\text{PVA}$ films, we poured the mixed solution comprising Bi_2Se_3 NPs and PVA powders into a standard cell and then dried it in an oven for two days. The $\text{Bi}_2\text{Se}_3/\text{PVA}$ films with different transmittance and color were deposited at different locations as shown in Fig. 3(a). Generally, the light and dark $\text{Bi}_2\text{Se}_3/\text{PVA}$ films with high and low transmittance were deposited on the upper and lower positions of the cell. The transmission spectrum of the dark and light $\text{Bi}_2\text{Se}_3/\text{PVA}$ film [Fig. 3(b) and (c)] was measured by the spectrum meter (NIRQUEST512-2.2, Ocean optics Inc.) within near- to mid-IR (900–2100 nm) by using a Halogen lamp (DH2000BAL, Ocean Optics Inc.) as the light source. The insets of Fig. 3(b) and (c) show photographs of these two films. Generally, the variation of the transmittance of these two films from near- to mid-IR are not obvious. The figures indicate that the transmittance of dark and light $\text{Bi}_2\text{Se}_3/\text{PVA}$ film is 18.9% and 75.5% at 1040 nm (corresponding 7.24 and 1.22 dB insertion loss), respectively.

After insertion of the dark $\text{Bi}_2\text{Se}_3/\text{PVA}$ film inside the cavity of YDFL, the stable Q-switched pulses were achieved as the pump power (P_{pump}) above a certain threshold. As the P_{pump} increased from 105.0 to 182.5 mW, the optical spectra of the Q-switched pulse at the corresponding output power from 2.1 to 4.6 mW are shown in Fig. 4(a)–(d). The plots depict that the central wavelength of the Q-switched YDFL is around 1036 nm. In addition, multiple emission peaks emerged on the top of the optical spectrum as a result of multiple interference of the $\text{Bi}_2\text{Se}_3/\text{PVA}$ film due to the etalon effect. Besides, the corresponding time traces of the consecutive Q-switched pulses are shown in Fig. 4(e)–(h). The plots reveal that the period of Q-switched pulses declines from 11.6 μs to 7.2 μs , and the repetition rate increases from 86.2 to 137.8 KHz as the pump power increases.

Fig. 5 shows the measured average output power (P_{out}) and the estimated pulse energy (E_{out}) of the YDFL as a function of the pump power in operation at the Q-switched state. In Fig. 5(a), the P_{out} (navey square) increased linearly with the P_{pump} and revealed the maximum value of about 4.6 mW with the P_{pump} at 182.5 mW. In Fig. 5(b), the repetition rate (R_{rep} , navey squares) of the Q-switched pulse increased from 86.2 to 137.8 KHz as the P_{pump} increased from 105 mW to

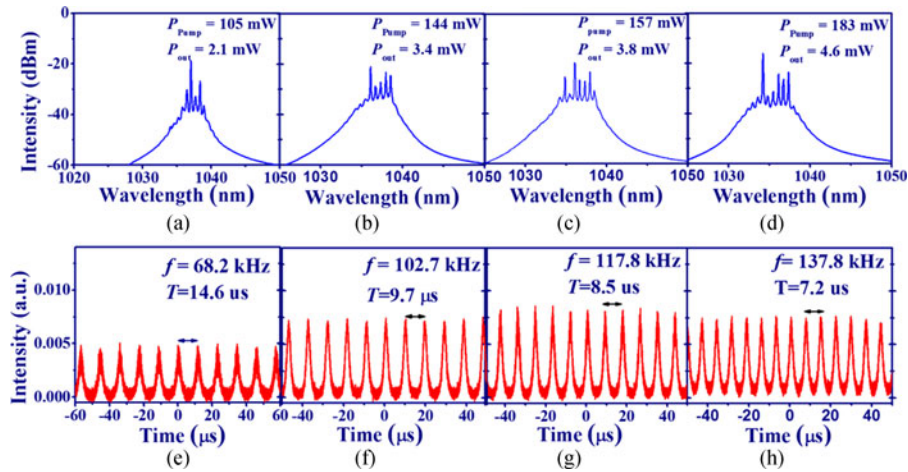


Fig. 4. (a)-(b) Optical spectra and (e)-(h) corresponded time trace of Q-switched pulses from YDFL by the dark $\text{Bi}_2\text{Se}_3/\text{PVA}$ film as the pump power increases from 105 mW to 182.5 mW.

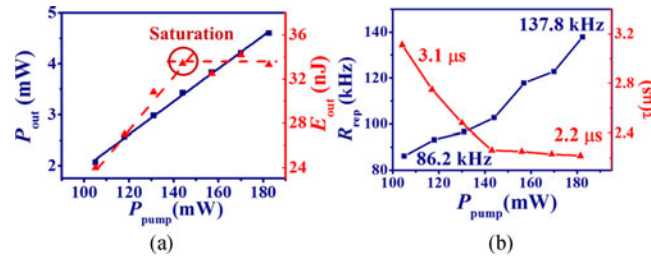


Fig. 5. (a) Average output power (P_{out}) and pulse energy (E_{out}) as well as (b) repetition rate (R_{rep}) and duration (τ) of Q-switched YDFL as a function of the pump power (P_{pump}).

182.5 mW. However, the duration (τ) of the Q-switched pulse declined quickly from 3.1 to 2.3 μs as the P_{pump} increased from 105 to 144 mW, but the declining rate of duration slowed down when the P_{pump} exceeded 140 mW. The shortest duration of about 2.2 μs was achieved when the P_{pump} was at 182.5 mW. Considering the output power and repetition rate of the Q-switching envelope, the pulse energy (E_{out}) of the Q-switched envelope can be obtained as shown by the red triangles in Fig. 5(a). The estimated E_{out} revealed the linearly increasing trend at lower pump power, but it was saturated when the P_{pump} was above 144 mW. The maximum E_{out} of about 34.2 nJ was obtained with $P_{\text{pump}} = 170$ mW. When the P_{pump} was above 182.5 mW, the Q-switched pulses became unstable and even disappeared. However, stable Q-switched operation can be observed again after we lowered the P_{pump} to 182.5 mW. This indicates that the $\text{Bi}_2\text{Se}_3/\text{PVA}$ film was not damaged by the thermal accumulation at high pump power.

The schematic setup to obtain the nonlinear absorption of the as-prepared $\text{Bi}_2\text{Se}_3/\text{PVA}$ film is shown in Fig. 6(a). The amplified PML-YDFL, with output pulses having repetition rate, pulsewidth, and a wavelength of about 19.6 MHz, 16 ps, and 1033 nm, was used as a light source. We applied a tunable attenuator in free space to vary the intensity of the ML pulse onto the SA. A 50/50 coupler was used to divide the input pulses into two fibers with almost identical strength. One beam transmitted through the SA, which was sandwiched between the two fiber connector, and then was detected by a photodiode. The other beam was directly measured by the other photodiode as a reference signal. These two detectors were connected with power meters to reveal the power. Owing to the absorption of the $\text{Bi}_2\text{Se}_3/\text{PVA}$ film, the transmitted light through the sample is slightly lower than that from the reference arm. The transmittance of $\text{Bi}_2\text{Se}_3/\text{PVA}$ film was obtained through

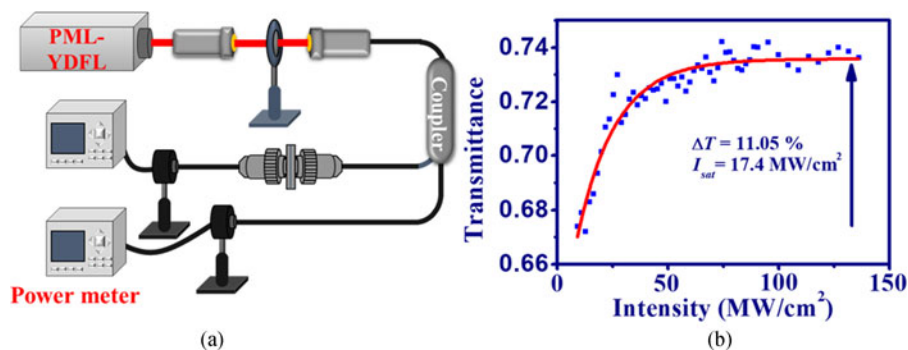


Fig. 6. (a) Schematic diagram of the experimental setup for transmittance measurement of SAs. (b) The nonlinear saturable absorption curve of the light $\text{Bi}_2\text{Se}_3/\text{PVA}$ film.

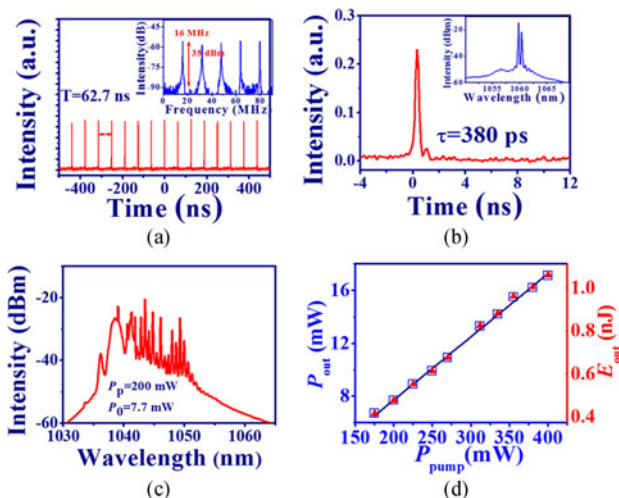


Fig. 7. (a) Time trace of mode-locked pulses (Inset shows the RF spectrum), (b) expanded single mode-locked pulse trace (Inset shows the optical spectrum of YDFL in operation at CW state), (c) corresponding spectrum of YDFL in operation at the mode-locked state as P_{pump} at 200 mW, and (d) average output power (P_{out}) and single pulse energy (E_{out}) versus pump power.

the division of the transmitted power of the sample by the reference power. Fig. 6(b) showed the transmittance of the pulsed light through the $\text{Bi}_2\text{Se}_3/\text{PVA}$ film as a function of light intensity. It was obvious to see the absorption saturation of the film at certain intensity of pulsed light that can be fitted by the equation

$$T(I) = 1 - \Delta T \cdot \exp\left(\frac{-I}{I_{\text{sat}}}\right) - T_{\text{ns}}, \quad (1)$$

where $T(I)$ and ΔT are the transmittance and modulation depth of SA, I and I_{sat} represent the intensity and the saturation intensity of pump pulse, and T_{ns} is the non-saturable loss. After fitting by (1) with the red curve shown in Fig. 6(b), the parameters ΔT , T_{ns} and I_{sat} of about 11.05%, 26.4%, and 17.4 MW/cm^2 , respectively, can be obtained. In comparison with previous results [27], the lower saturable intensity of the produced $\text{Bi}_2\text{Se}_3/\text{PVA}$ film in this work could reduce the threshold pump power of mode-locked lasers.

If we inserted the light $\text{Bi}_2\text{Se}_3/\text{PVA}$ film inside the cavity of the YDFL, the stable mode-locked pulses were generated as P_{pump} increased from 175 mW to 400 mW. The time trace of the ML pulses in Fig. 7(a) shows that the period of the ML pulse is about 62.7 ns, which corresponds to

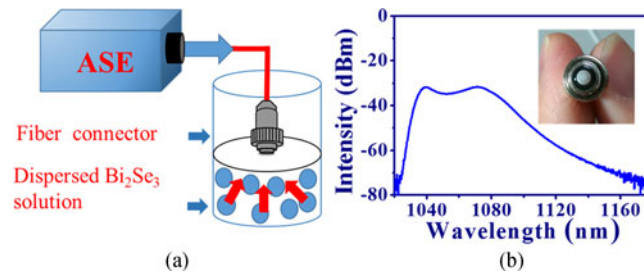


Fig. 8. (a) Schematic setup to reveal the deposition of Bi_2Se_3 NPs onto the end facet of fiber, and (b) the spectrum of ASE light. (Inset: the picture of the end facet of fiber with TI NPs.)

the pulse repetition rate of about 16 MHz as shown in the RF spectrum (Inset of Fig. 7(a)). Thus, the cavity length of YDFL is estimated to be about 12.5 m. The RF spectrum also indicates that the signal to noise ratio is about 35 dBm. When the P_{pump} reached 200 mW, the time trace and optical spectrum of the ML pulse are shown in Fig. 7(b) and (c). The zoom in time trace of the single ML trace in Fig. 7(b) indicates that the pulsewidth of the ML pulse is about 380 ps. As the YDFL is operation at continuous wave (CW) state, several narrow emission peaks around 1060 nm were revealed as shown in the inset of Fig. 7(c) because of the mode competition. Once the YDFL is mode-locked, a broad spectrum can be revealed in Fig. 7(c), in which the peak wavelength of the soliton is around 1038.5 nm. In addition, many oscillation modes will be excited within the long wavelength range at high pump power. However, the mode-locked pulses can only be sustained within one hour. Fig. 7(d) shows the measured average output power (P_{out} , blue square) and the corresponding pulse energy (E_{out} , red triangle) as a function of the pump power. In Fig. 7(d), the P_{out} and E_{out} increase linearly with the P_{pump} and the maximum P_{out} of about 17.1 mW can be obtained with the P_{pump} at 400 mW. The estimated E_{out} increases from 0.41 to 1.06 nJ as the P_{pump} increases from 175 to 400 mW.

3.2 Short Pulse Generation by Bi_2Se_3 Compatible Fiber

In comparison with the $\text{Bi}_2\text{Se}_3/\text{PVA}$ film, the TI compatible fiber can be applied to the PML-YDFL to produce more stabilized ML pulses owing to its better thermal property. In order to produce the Bi_2Se_3 compatible fiber, the Bi_2Se_3 dispersed solution was diluted two times by adding 15 ml DI water into 15 ml produced Bi_2Se_3 solution, and was processed using ultrasonication for 10 minutes. Before optical deposition, the diluted Bi_2Se_3 solution was ultra-agitated for 10 minutes to lead to a homogenous distribution of the Bi_2Se_3 NPs in solution (Inset of Fig. 9(a)). An amplified spontaneous emission (ASE) light source with 20 mW output power, by using ytterbium doped fiber as the gain medium (YFAS4BB128006A, GIP Inc), was connected to one end of the standard SMF (HI1060) and the other facet of SMF was immersed into the diluted Bi_2Se_3 solution as shown in Fig. 8(a). After an hour deposition, the Bi_2Se_3 NPs were gradually deposited onto the end facet of the fiber core as shown in the inset of Fig. 8(b). Then, we dried the fiber end facet in an oven with a temperature of 40 °C for 3 hours.

The transmission spectrum of the bare fiber (red solid curve) and TI compatible SA (blue solid curve) are shown in Fig. 9(a). The figure indicates that the bare fiber revealed high transmittance of above 95% within 1030–1100 nm, and declined obviously after TI NPs were deposited onto the end facet of fiber. The picture of the diluted Bi_2Se_3 solution was shown in the left inset of Fig. 9(a) and the right inset of Fig. 9(a) shows the deposited NPs onto the end facet of the fiber core. The measured transmittance T_0 of TI-compatible fiber was around 44.8% at 1040 nm (corresponding 3.5 dB insertion loss). Fig. 9(b) shows the nonlinear saturable absorption curve of the Bi_2Se_3 compatible fiber as a function of light intensity with the central wavelength of 1047 nm. The nonlinear transmittance of the Bi_2Se_3 compatible fiber can be well fitted by (1) (red solid curve in Fig. 9(b)) to obtain the parameters of ΔT , T_{ns} and I_{sat} of 9.2%, 76%, and 14.9 MW/cm², respectively.

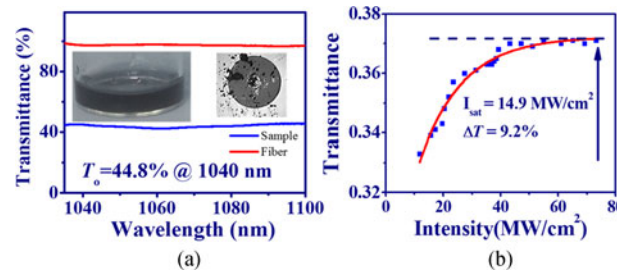


Fig. 9. (a) Transmittance of the bare fiber (red line) and Bi_2Se_3 compatible fiber (blue line). (Left inset: The produced Bi_2Se_3 dispersive solution in a small vessel. Right inset: The side view of Bi_2Se_3 NPs on the end facet of fiber). (b) The nonlinear saturable absorption curve of the Bi_2Se_3 compatible fiber.

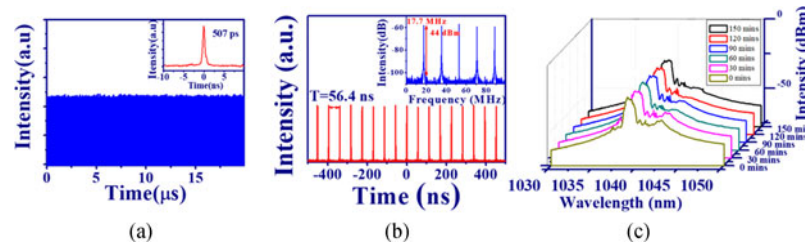


Fig. 10. (a) Time trace of the mode-locked pulse from YDFL by the Bi_2Se_3 compatible fiber (Inset shows the expanded single mode locked pulse train), (b) time trace of mode-locked pulse trains (Inset shows the RF spectrum), and (c) recorded optical spectra measured every 30 minutes.

The non-saturable loss of the TI-compatible fiber of around 76% was primarily due to the scattering and absorption of Bi_2Se_3 NPs.

In comparison with the $\text{Bi}_2\text{Se}_3/\text{PVA}$ film, the concentration of deposited Bi_2Se_3 NPs onto the end facet of fiber is slightly high. It would induce stronger absorbance as the pulsed light passed through Bi_2Se_3 compatible fiber than the $\text{Bi}_2\text{Se}_3/\text{PVA}$ film and caused the increase of insertion loss. Thus, the transmittance of TI compatible fiber in Fig. 9(a) is lower than that from $\text{Bi}_2\text{Se}_3/\text{PVA}$ film in Fig. 3(c). However, the mode-locked pulses can be generated at low pump power of about 75 mW in Bi_2Se_3 compatible fiber. In previous report [30], the threshold energy (E_p) for the ML pulse generation in laser system was estimated by the formula:

$$E_p^2 > E_{\text{sat,L}} E_{\text{sat,A}} \Delta R. \quad (2)$$

Here, $E_{\text{sat,L}}$ and $E_{\text{sat,A}}$ are the saturation energy of the gain and absorber, and ΔR is the modulation depth of the SA. Owing to the larger modulation depth about (ΔR) 11.05% from $\text{Bi}_2\text{Se}_3/\text{PVA}$ film in Fig. 6(b) than that from Bi_2Se_3 compatible fiber with $\Delta R \sim 9.2\%$ in Fig. 9(b), the mode-locked threshold of YDFL using $\text{Bi}_2\text{Se}_3/\text{PVA}$ film is higher. With $P_{\text{pump}} = 75$ mW, the time trace of the ML pulse trains is shown in Fig. 10(a). In this operation state, the output power and corresponded pulse energy are around 1.88 mW and 0.1 nJ, respectively. The inset of Fig. 10(a) indicates that the pulsewidth of the ML pulse was around 507 ps. In addition, the period of mode-locked pulse around 56.4 ns was revealed in Fig. 10(b) that corresponded to the repetition rate of around 17.7 MHz. It also revealed a little bit higher signal to noise rate about 44 dBm than the mode-locked state by using the $\text{Bi}_2\text{Se}_3/\text{PVA}$ film (Inset of Fig. 7(b)). Once the YDFL was mode-locked, a spectrum with the central wavelength of the soliton of around 1039 nm and the 3-dB bandwidth of around 1.4 nm can be produced. In order to test the stability of the mode-locked pulses, we continuously monitored the output spectra of the PML-YDFL for 2.5 hours as shown in Fig. 10(c). It showed that the variation in the central wavelength was around 1039 nm and the 3-dB bandwidth was around 1.4 ± 0.036 nm, which confirmed the relatively stable operation of the mode-locked pulses when using the Bi_2Se_3 compatible fiber.

4. Conclusion

In this work, the Q-switched pulse and mode-locked pulse in an all-normal dispersion Yb-doped fiber laser were demonstrated based on the topological insulator Bi_2Se_3 synthesized via a polyol method as a saturable absorber. Then, Bi_2Se_3 /PVA films with high and low transmittance were deposited at top and bottom locations of the standard cell by drying the mixed solution comprising Bi_2Se_3 NPs and PVA powders. Through the dark Bi_2Se_3 /PVA film in the laser cavity, the Q-switched pulses from YDFL could be generated to reveal a maximum pulse energy of about 34.2 nJ at 170 mW pump power. As the pump power increased from 105 to 182 mW, the repetition rate of the Q-switched pulses increased from 86.2 kHz to 137.8 kHz, but the duration was decreased from 3.1 μs to 2.2 μs . On the contrary, the mode-locked pulses with 16 MHz repetition rate and the shortest pulsewidth of about 380 ps could be generated using the light Bi_2Se_3 /PVA film. From nonlinear transmittance measurement, the modulation depth of the light Bi_2Se_3 /PVA film was 11.05%, and the saturation intensity was 17.4 MW/cm². In addition, the Bi_2Se_3 compatible fiber was also produced by deposition of Bi_2Se_3 nano-platelets on the end facet of the fiber. Through the nonlinear absorption measurement, it showed a modulation depth of 9.2% and a saturation intensity of 14.9 MW/cm². In comparison with the Bi_2Se_3 /PVA film, the low pump power of about 75 mW is sufficient to produce the mode-locked pulse with long-term operation of about 2.5 hours.

Acknowledgment

The authors would like to thank Dr. Y.-C. Chuang at NSRRC for the XRD measurement of Bi_2Se_3 NPs.

References

- [1] J.-H. Lin, C. L. Chen, C.-W. Chan, and Y.-H. Chen, "Investigation of noise-like pulses from a net normal Yb-doped fiber laser based on a nonlinear polarization rotation mechanism," *Opt. Lett.*, vol. 41, pp. 5310–5313, Nov. 2016.
- [2] J.-H. Lin, C.-W. Chan, H.-Y. Lee, and Y.-H. Chen, "Bound states of dispersion-managed solitons from single-mode Yb-doped fiber laser at net-normal dispersion," *IEEE Photon. J.*, vol. 7, no. 5, Oct. 2015, Art. no. 7102409.
- [3] W.-C. Chang *et al.*, "Investigation of Q-switched and mode-locked pulses from a Yb³⁺-doped germano-zirconia silica glass based fiber laser," *IEEE Photon. J.*, vol. 9, no. 4, Aug. 2017, Art. no. 7104708.
- [4] H. Chen, S. P. Chen, Z. F. Jiang, and J. Hou., "0.4 μJ , 7 kW ultrabroadband noise-like pulse direct generation from an all-fiber dumbbell-shaped laser," *Opt. Lett.*, vol. 40, no. 23, pp. 5490–5493, 2015.
- [5] K.-H. Lin, J.-H. Lin, and C.-C. Chen, "Switchable mode-locking states in an all-fiber all-normal-dispersion ytterbium-doped laser," *Laser Phys.*, vol. 20, pp. 1984–1989, 2010.
- [6] M. Jung, J. Koo, Y. M. Chang, P. Debnath, Y.-W. Song, and J. H. Lee, "An all fiberized, 1.89- μm Q-switched laser employing carbon nanotube evanescent field interaction," *Laser Phys. Lett.*, vol. 9, pp. 669–673, 2012.
- [7] Z. Sun *et al.*, "Graphene mode-locked ultrafast laser," *ACS Nano*, vol. 4, pp. 803–810, 2010.
- [8] Y. Cui and X. Liu, "Graphene and nanotube mode-locked fiber laser emitting dissipative and conventional solitons," *Opt. Exp.*, vol. 21, no. 16, pp. 18969–18974, 2013.
- [9] M. Jung *et al.*, "Mode-locked pulse generation from an all-fiberized, Tm-Ho-codoped fiber laser incorporating a graphene oxide-deposited side-polished fiber," *Opt. Exp.*, vol. 21, pp. 20062–20072, 2013.
- [10] J. Lee, J. Koo, P. Debnath, Y.-W. Song, and J. H. Lee, "A Q-switched, mode-locked fiber laser using a graphene oxide-based polarization sensitive saturable absorber," *Laser Phys. Lett.*, vol. 10, 2013, Art. no. 035103.
- [11] G. Sobon, "Mode-locking of fiber lasers using novel two-dimensional nanomaterials: Graphene and topological insulators," *Photon. Res.*, vol. 3, no. 2, pp. A56–A63, 2015.
- [12] X. Li *et al.*, "Single-wall carbon nanotubes and graphene oxide-based saturable absorbers for low phase noise mode-locked fiber lasers," *Sci. Rep.*, vol. 6, 2016, Art. no. 25266.
- [13] H. Yu *et al.*, "Topological insulator as an optical modulator for pulsed solid-state lasers," *Laser Photon. Rev.*, vol. 7, no. 6, pp. L77–L83, 2013.
- [14] H. Zhang, C. X. Liu, X. L. Qi, X. Dai, Z. Fang, and S. C. Zhang, "Topological insulators in Bi_2Se_3 , Bi_2Te_3 and Sb_2Te_3 with a single Dirac cone on the surface," *Nature Phys.*, vol. 5, no. 6, pp. 438–442, 2009.
- [15] Y. L. Chen *et al.*, "Experimental realization of a three-dimensional topological insulator, Bi_2Te_3 ," *Science*, vol. 325, no. 5937, pp. 178–181, 2009.
- [16] Y. Xia *et al.*, "Observation of a large-gap topological-insulator class with a single Dirac cone on the surface," *Nature Phys.*, vol. 5, no. 6, pp. 398–402, 2009.
- [17] C. Chi, J. Lee, J. Koo, and J. H. Lee, "All-normal-dispersion dissipative-soliton fiber laser at 1.06 μm using a bulk-structured Bi_2Te_3 topological insulator-deposited side-polished fiber," *Laser Phys.*, vol. 24, no. 10, 2014, Art. no. 105106.
- [18] Z. Q. Luo *et al.*, "Topological-Insulator passively Q-switched double-clad fiber laser at 2 μm wavelength," *IEEE J. Sel. Top. Quantum*, vol. 20, no. 5, Sep./Oct. 2014, Art. no. 0902708.

- [19] J. Lee, J. Koo, Y. M. Jhon, and J. H. Lee, "A femtosecond pulse erbium fiber laser incorporating a saturable absorber based on bulk-structured Bi_2Te_3 topological insulator," *Opt. Exp.*, vol. 22, no. 5, pp. 6165–6173, 2014.
- [20] J. Sotor, G. Sobon, W. Macherzynski, P. Paletko, K. Grodecki, and K. M. Abramski, "Mode-locking in Er-doped fiber laser based on mechanically exfoliated Sb_2Te_3 saturable absorber," *Opt. Mater. Exp.*, vol. 4, no. 1, pp. 1–6, 2014.
- [21] B. Guo *et al.*, "Observation of bright-dark soliton pair in a fiber laser with topological insulator," *IEEE Photon. Tech. Lett.*, vol. 27, no. 7, pp. 701–704, Apr. 2015.
- [22] B. Guo *et al.*, "Dual-wavelength rectangular pulse erbium-doped fiber laser based on topological insulator saturable absorber," *Photon. Res.*, vol. 3, no. 3, pp. 94–99, 2015.
- [23] C. Zhao *et al.*, "Wavelength-tunable picosecond soliton fiber laser with topological insulator: Bi_2Se_3 as a mode locker," *Opt. Exp.*, vol. 20, no. 25, pp. 20888–27895, 2012.
- [24] H. Liu *et al.*, "Femtosecond pulse generation from a topological insulator mode-locked fiber laser," *Opt. Exp.*, vol. 22, no. 6, pp. 6868–6873, 2014.
- [25] Z. Yu *et al.*, "High-repetition-rate Q-switched fiber laser with high quality topological insulator Bi_2Se_3 film," *Opt. Exp.*, vol. 22, no. 10, pp. 11508–11515, 2014.
- [26] H. Ahmad, M. R. K. Itanian, L. Narimani, I. S. Amiri, A. Khodaei, and S. W. Harun, "Tunable S-band Q-switched fiber laser using Bi_2Se_3 as the saturable absorber," *IEEE Photon. J.*, vol. 7, no. 3, pp. 1–8, Jun. 2015, Art. no. 1502508.
- [27] Y. Chen *et al.*, "Self-assembled topological insulator: Bi_2Se_3 membrane as a passive Q-switcher in an erbium-doped fiber laser," *J. Lightw. Technol.*, vol. 31, no. 17, pp. 2857–2863, Sep. 2013.
- [28] Z. Q. Luo *et al.*, "1.06 μm Q-switched ytterbium-doped fiber laser using few-layer topological insulator Bi_2Se_3 as a saturable absorber," *Opt. Exp.*, vol. 21, no. 24, pp. 29516–29522, 2013.
- [29] Z. Dou, Y. Song, J. Tian, J. Liu, Z. Yu, and X. Fang, "Mode-locked ytterbium-doped fiber laser based on topological insulator: Bi_2Se_3 ," *Opt. Exp.*, vol. 22, no. 20, pp. 24055–24061, 2014.
- [30] C. Honninger, R. Paschotta, F. Morier-Genoud, M. Moser, and U. Keller, "Q-switching stability limits of continuous-wave passive mode locking," *J. Opt. Soc. Amer. B*, vol. 16, no. 1, pp. 46–56, 1999.